Inorganic Chemistry

Article

pubs.acs.org/IC

Magnetic Interactions Mediated by Diamagnetic Cations in [$Mn_{18}M$] (M = Sr^{2+}, Y^{3+}, Cd^{2+}, and Lu^{3+}) Coordination Clusters

Ayuk M. Ako,*[,†] Boris Burger,[†] Yanhua Lan,[†] Valeriu Mereacre,[†] Rodolphe Clérac,*[,‡,§] Gernot Buth,[⊥] Silvia Gómez-Coca,[¶] Eliseo Ruiz,*[,¶] Christopher E. Anson,[†] and Annie K. Powell*[,†,∥]

[†]Institut für Anorganische Chemie, Karlsruhe Institute of Technology, Engesserstr. 15, D-76131, Karlsruhe, Germany

[‡]CNRS, CRPP, UPR 8641, F-33600 Pessac, France

[§]Univ. Bordeaux, CRPP, UPR 8641, F-33600 Pessac, France

[⊥]Institut für Synchrotronstrahlung, Karlsruhe Institute of Technology, D-76344 Eggenstein-Leopoldshafen, Germany

[¶]Departament de Química Inorgànica and Institut de Recerca de Química Teòrica i Computacional, Universitat de Barcelona, Diagonal 645, 08028 Barcelona, Spain

[∥]Institute of Nanotechnology, Karlsruhe Institute of Technology, D-76131, Karlsruhe, Germany

Supporting Information

ABSTRACT: We previously reported how the synthesis of $[Mn^{III}_{12}Mn^{II}_{7}(\mu_4\text{-}O)_8(\mu_3\text{-}\eta^1\text{-}N_3)_8(HL^1)_{12}(MeCN)_6]Cl_2\cdot 10MeOH\cdot MeCN$ (**1**), which has a Mn_{19} core corresponding to two supertetrahedral $\{Mn^{II}_4Mn^{III}_6\}$ units sharing a common Mn^{II} vertex, can be modified such that the central octacoordinate Mn^{II} ion can be replaced by metal ions more likely to favor this coordination geometry such as Dy^{III} as exemplified in the compound $[Mn^{III}_{12}Mn^{II}_6Dy^{III}(\mu_4\text{-}O)_8(\mu_3\text{-}Cl)_{6.5}(\mu_3\text{-}N_3)_{1.5}(HL)_{12}(MeOH)_6]Cl_3\cdot 25MeOH$ (**2**). Here, we report a systematic survey of the effects of incorporating various diamagnetic metal ions $\mathbf{M}^{n+}$ into this central position. We chose diamagnetic ions with electron configurations with fully occupied or completely empty frontier orbitals in order to gauge the effect on the overall magnetic behavior. The syntheses, structures, and magnetic properties of the heterometallic aggregates $[Mn^{III}_{12}Mn^{II}_6Sr^{II}(\mu_4\text{-}O)_8(\mu_3\text{-}\eta^1\text{-}N_3)_{7.5}(\mu_3\text{-}\eta^1\text{-}Cl)_{0.5}(HL^1)_{12}(MeCN)_6]Cl_2\cdot 15MeOH$ (**3**), $[Mn^{III}_{12}Mn^{II}_6Y^{III}(\mu_4\text{-}O)_8(\mu_3\text{-}\eta^1\text{-}N_3)_8(HL^1)_{12}(MeCN)_6](NO_3)_3\cdot 11MeOH$ (**4**), $[Mn^{III}_{12}Mn^{II}_6Cd^{II}(\mu_4\text{-}O)_8(\mu_3\text{-}\eta^1\text{-}N_3)_{6.8}(\mu_3\text{-}\eta^1\text{-}Cl)_{1.2}(HL^1)_{12}(MeCN)_6](CdCl_4)_{0.25}Cl_{1.5}\cdot 14.5MeOH$ (**5**), and $[Mn^{III}_{12}Mn^{II}_6Lu^{III}(\mu_4\text{-}O)_8(\mu_3\text{-}\eta^1\text{-}N_3)_{6.5}(\mu_3\text{-}\eta^1\text{-}Cl)_{1.5}(HL^2)_{12}(MeCN)_6]Cl_3\cdot 3H_2O\cdot 7MeOH\cdot MeCN$ (**6**) (H_3L^1 = 2,6-*bis*(hydroxymethyl)-4-methylphenol, H_3L^2 = 2,6-*bis*(hydroxymethyl)-4-fluorophenol) are reported. The aggregates were prepared in one-pot self-assembly reactions of H_3L^1 (or H_3L^2), $MnCl_2\cdot 4H_2O$ or $Mn(NO_3)_2\cdot 4H_2O$, $NaOAc\cdot 3H_2O$ or Et_3N, and NaN_3 in the presence of the appropriate diamagnetic metal salt in MeCN/MeOH mixtures. Compounds **3**–**6** crystallize isotypically to **1** in the trigonal space group $R\bar{3}$ with $Z = 3$. The effects on the magnetic properties were investigated, paying attention to the presence of any weak coupling mediated by the diamagnetic cations between the two $\{Mn^{II}_3Mn^{III}_6\}$ $S = 39/2$ subunits. In the Cd^{2+} compound **5**, the two $\{Mn^{II}_3Mn^{III}_6\}$ units are magnetically isolated. In **3**, **4**, and **6**, the diamagnetic Sr^{2+}, Y^{3+}, and Lu^{3+} cations mediate weak antiferromagnetic interactions between the two $\{Mn^{II}_3Mn^{III}_6\}$ subunits. DFT calculations show that the inter-$\{Mn^{II}_3Mn^{III}_6\}$ interactions in the $Mn_{18}\mathbf{M}$ systems are attributable to the electronic structure of the central diamagnetic cation, with systems containing trivalent central cations showing stronger antiferromagnetic interactions than those with isoelectronic divalent cations.

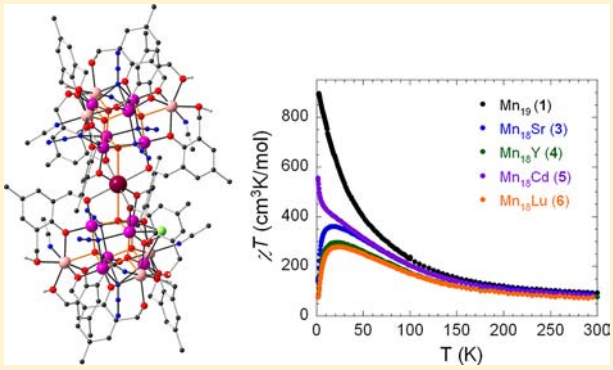

INTRODUCTION

The directed synthesis of high-nuclearity coordination clusters in which the core has a specified structural topology remains a very challenging synthetic goal. Nevertheless, certain motifs and topologies appear to be in some way favorable. This is especially so for the widely investigated manganese-based coordination clusters, which can serve both as models for various metalloenzymes[1] as well as show interesting magnetic properties, including that of single molecule magnet properties.[2] Among the relatively well-defined core topologies seen for these manganese-based systems is that of the mixed-valent supertetrahedron motif $\{Mn^{II}_4Mn^{III}_6\}$ in which a large tetrahedron of four Mn^{II} ions has an octahedron of six Mn^{III} ions inscribed within it such that each Mn^{III} ion is placed halfway along each of the six edges of the supertetrahedron. So far, this unit has been characterized structurally and magnetically as an isolated unit,[3] where the overall ferromagnetic

Received: November 22, 2012
Published: May 7, 2013

 © 2013 American Chemical Society dx.doi.org/10.1021/ic3025588 | *Inorg. Chem.* 2013, 52, 5764–5774

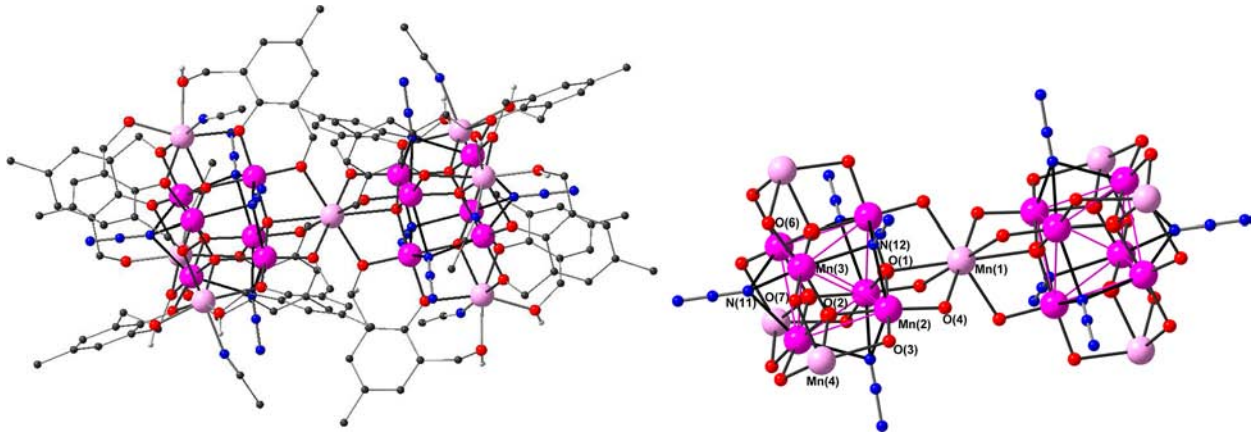

Figure 1. Molecular structure of **1** (left); Mn_{19} core of **1** showing (μ_3-N_3) ligands and oxygen bridges (right). Reprinted with permission from ref 4. Copyright 2006 John Wiley & Sons, Inc. (Mn^{III}: purple; Mn^{II}: pink; O: red; N: blue; C: dark gray).

coupling giving a spin ground state of $S = 22$ within the motif was clear, as well as in systems where two such supertetrahedral building blocks can be joined by a common vertex[4,5] or a common edge.[6] Although the ferromagnetic coupling within the isolated supertetrahedral unit appears to remain inviolate, the precise geometrical details of the way in which two such units are joined together exert a subtle influence on the resulting ground spin state. For example, in our previously reported vertex-sharing $[Mn_{19}]$-aggregate $[Mn^{III}_{12}Mn^{II}_{7}(\mu_4\text{-}O)_8(\mu_3\text{-}\eta^1\text{-}N_3)_8(HL^1)_{12}(MeCN)_6]Cl_2\cdot 10MeOH\cdot MeCN$ (**1**), the system is completely ferromagnetically coupled to give a record spin ground state of $S = 83/2$.[4] On the other hand, the topologically similar $[Mn_{19}]$-aggregate isolated by Kou et al. was found to display a lower spin ground state of $S = 73/2$.[5] This can be rationalized if it is assumed that, within what we can formulate as the $[\{Mn^{II}_3Mn^{III}_6\}_2\mathbf{M}]$ core motif, the spin on the common vertex-sharing central **M** linking the two supertetrahedral motifs (here **M** = Mn^{II}) is aligned to be antiparallel (rather than parallel as found in **1**) to the two giant spin $S = 39/2$ states of the $\{Mn^{II}_3Mn^{III}_6\}$ units. Furthermore, the two examples in the literature of edge-sharing supertetrahedral $\{Mn_{17}\}$ aggregates also show different ground spin states, again indicating that the way in which two such supertetrahedral $\{Mn_{10}\}$ units are joined modulates the overall magnetic properties.[6] All these compounds show either no single molecule magnet (SMM) behavior or only a very weak slow relaxation of magnetization. However, their very high isotropic spins make them good candidates for magnetic refrigeration using the magnetocalorific effect.[7] Although the compounds incorporate the Jahn–Teller elongated Mn^{III} ion which should provide the uniaxial anisotropy required for SMM systems,[8] the octahedral arrangement leads to the cancellation of the single-ion zero-field splitting, D, contributions to the overall molecular D value.[9]

Another relevant structural feature of **1** (Figure 1) is the unusual 8-coordinate geometry about the central Mn^{II}, Mn(1), which has an $\{O_8\}$ donor set with relatively long[10] Mn(1)-O bond lengths lying in the range of 2.344–2.509 Å. This suggests that the oxygen atoms are relatively weakly bound to Mn(1). Furthermore, DFT calculations[11] on the $\{Mn_{19}\}$ aggregate (**1**) revealed that the length of the Mn(1)-O bonds is key to whether this central ion is ferromagnetically or antiferromagnetically coupled to the two $S = 39/2$ $\{Mn^{II}_3Mn^{III}_6\}$ subunits to give the $S_T = 83/2$ observed by us[4] and the $S_T = 73/2$ observed by Kou et al.,[5] respectively. It seemed reasonable that such a predestined 8-fold coordination environment would be more accommodating for larger metal cations such as those of the rare-earths which we successfully demonstrated in isolating the compound $[Mn^{III}_{12}Mn^{II}_6Dy^{III}(\mu_4\text{-}O)_8(\mu_3\text{-}Cl)_{6.5}(\mu_3\text{-}N_3)_{1.5}(HL)_{12}(MeOH)_6]Cl_3\cdot 25MeOH$ (**2**) where **M** = Dy^{III}.[12] The motivation for this was to see if it was possible to turn **1** into a single molecule magnet (SMM) (which it was) by adding a negative anisotropy D to the existing high ground state spin, S. We chose Dy^{III} since this ion can justifiably be regarded as having produced the largest number of interesting pure 4f and 3d-4f SMMs, as demonstrated in recent work by us and others exploring the fact that most lanthanide ions can provide both large and uniaxial spins[12−14] and demonstrating that 3d–4f coordination clusters can show useful SMM properties.[15−18] The key point in terms of the present study, however, is our finding that the simple addition of $Dy(NO_3)_3\cdot 6H_2O$ to the reaction mixture used to obtain original $\{Mn_{19}\}$ aggregate **1** allowed for the selective replacement of the central Mn^{II} in (**1**) with the anisotropic Dy^{III} ion to yield compound **2**.[12] This led us to the idea of investigating whether other **M** ions could be captured in this site between the two $S = 39/2$ $\{Mn^{II}_3Mn^{III}_6\}$ moieties. Furthermore, it is of interest to explore capturing suitably sized full or empty shell ions with s, p, or d frontier orbitals in order to investigate the effect on the overall magnetic behavior. This makes it possible to test whether the nature of filled or empty frontier orbitals affects the degree of communication between the two $S = 39/2$ $\{Mn^{II}_3Mn^{III}_6\}$ units. This is analogous to gauging the ability of various closed-shell ions, such as oxides, hydroxides, sulfides, fluorides, chlorides and so on, to mediate magnetic superexchange between isolated metal ions. Now, however, we are investigating the ability of closed shell metal ions to mediate superexchange between two giant spin ($S = 39/2$) coordination cluster units. Here, we report the synthesis and characterization of the heterometallic $[Mn_{18}\mathbf{M}]$ coordination clusters where **M** = Sr^{2+}, **3**; Y^{3+}, **4**; Cd^{2+}, **5**; Lu^{3+}, **6**.

A major goal of this study was to probe the structural and electronic flexibility of the $\{Mn_{19}\}$ system using diamagnetic closed-shell ions Sr^{2+}, Y^{3+}, Cd^{2+}, and Lu^{3+} which differ in their electronic configurations and charges. For example, Sr^{2+} and Y^{3+} are both isoelectronic with Kr, with the outermost shell containing filled $4s^24p^6$ orbitals, but with different ionic charge and radius. However, there is also the question of what effect the proximity of empty 4d orbitals may have on the magnetic interaction between the two $S = 39/2$ $\{Mn^{II}_3Mn^{III}_6\}$ units.

dx.doi.org/10.1021/ic3025588 | Inorg. Chem. 2013, 52, 5764–5774

Cd^{2+}, with the configuration $[Kr]4d^{10}$, has an additional full shell of 4d-electrons compared with Sr^{2+} and Y^{3+}. The configuration for Lu^{3+} can be written as $[Kr]4d^{10}4f^{14}5s^25p^6$, in which the outermost filled orbitals ($5s^25p^6$) are similar in terms of the quantum numbers l to those of Sr^{2+} and Y^{3+} ($4s^24p^6$) but not in terms of principal quantum number n and thus the accessibility of f orbitals. An important motivation for this study is that we wanted to test whether the practice of substituting paramagnetic 4f ions in 3d−4f systems with diamagnetic rare earth cation analogues, i.e., La^{3+}, Y^{3+}, or Lu^{3+}, in order to estimate the contribution to the magnetism from the 3d ions, is experimentally robust. We have noticed in our own work using this approach that such diamagnetic ions are capable of transmitting, albeit weakly, magnetic information between the 3d centers.[16] In the case of the $\{Mn^{II}_3Mn^{III}_6\}_2\mathbf{M}$ compounds, the very high $S = 39/2$ ground states of the $[Mn_9]$ units in compounds **3**−**6** should provide sufficiently large contributions to the magnetization to allow direct experimental determination of the magnitude of such interactions. The experimental results obtained can then be compared with DFT calculations carried out on these compounds. Furthermore, by analogy with closed-shell diamagnetic ions mediating magnetic interactions through superexchange (the bread-and-butter of metal oxide and molecule-based magnetic interactions), it should be possible that closed-shell metal ion species, given the correct energy levels of frontier orbitals and geometries, can provide superexchange pathways between the giant $S = 39/2$ spins of the $\{Mn^{II}_3Mn^{III}_6\}$ units.

EXPERIMENTAL SECTION

All reactions were carried out under aerobic conditions. Unless otherwise stated, all reagents were obtained from commercial sources and were used as received, without further purification. The synthesis of 2,6-*bis*(hydroxymethyl)-4-fluorophenol (H_3L^2) will be described elsewhere. Elemental analyses (CHN) were carried on dried samples using an Elementar Vario EL analyzer. The dried compounds were found to lose some of the lattice solvents and absorb some water. FTIR spectra were measured on a Perkin-Elmer Spectrum One spectrometer with samples prepared as KBr pellets. ***Caution!*** *Although no such tendency was observed during the present work, azide salts are potentially explosive and should be handled with care and in small quantities.*

Synthesis. *$[Mn^{III}_{12}Mn^{II}_6Sr(\mu_4\text{-}O)_8(\mu_3\text{-}Cl)_{0.5}(\mu_3\text{-}\eta^1\text{-}N_3)_{7.5}(HL^1)_{12}(MeCN)_6]Cl_2\cdot 15MeOH$ (**3**).* A slurry of $MnCl_2\cdot 4H_2O$ (0.4 g, 2 mmol), NaN_3 (0.2 g, 3 mmol), $NaO_2CMe\cdot 3H_2O$ (0.28 g, 2 mmol), and 2,6-bis(hydroxymethyl)-4-methylphenol (1.02 g, 6 mmol) in 25 mL of MeCN and 5 mL of MeOH was stirred for 30 min at room temperature; then, a solution of $Sr(NO_3)_2\cdot 6H_2O$ (0.21 g, 1.00 mmol) in 5 mL of MeCN was added. The resulting mixture was stirred for an additional 1 h and then heated at reflux for 2 h to afford a dark brown solution, which was cooled and filtered. Dark brown crystals of **3** were obtained after six days, washed with a small amount of MeCN, and dried in air. Yield: 26% (based on Mn). Elemental analysis (%) calc. for $C_{120}H_{180}Cl_{2.5}Mn_{18}N_{28.5}O_{65}Sr$ (**3**·21H_2O): C 34.10; H 4.30; N 9.44; found: C 34.09; H 4.15; N 9.48. Selected IR data (KBr pellet, cm^{-1}): 418 (w), 473 (m), 516 (m), 555 (s), 636 (s), 656 (s), 769 (w), 810 (m), 865 (w), 900 (vw), 952 (w), 983 (m), 997 (m), 1027 (m), 1161 (m), 1225 (m), 1253 (s), 1322 (m), 1349 (w), 1384 (m), 1470 (vs), 1613 (m), 2061 (vs, N_3), 2828 (m), 2881 (m), 2916 (m), 3002 (m), 3355 (s, br).

*$[Mn^{III}_{12}Mn^{II}_6Y^{III}(\mu_4\text{-}O)_8(\mu_3\text{-}\eta^1\text{-}N_3)_8(HL^1)_{12}(MeCN)_6](NO_3)_3\cdot 11MeOH$ (**4**).* A slurry of $Mn(NO_3)_3\cdot 4H_2O$ (0.36 g, 2 mmol), NaN_3 (0.2 g, 3 mmol), Et_3N (0.6 g, 6 mmol), and 2,6-bis(hydroxymethyl)-4-methylphenol (1.02 g, 6. mmol) in 25 mL of MeCN and 5 mL of MeOH was stirred for 30 min at room temperature, and then, a solution of $Y(NO_3)_3\cdot 6H_2O$ (0.38 g, 1 mmol) in 5 mL of MeCN was added. The resulting mixture was stirred for an additional 1 h and then heated at reflux for 2 h to afford a dark brown solution, which was cooled and filtered. Dark brown crystals of **4** were obtained within a few days. Yield: 21% (based on Mn). Elemental analysis (after drying in vacuo) (%) calcd for $C_{120}H_{138}Mn_{18}N_{33}O_{53}Y$ (solvent free): C 36.32; H 3.50; N 11.64; found: C 36.15; H 3.65; N 11.82. Selected IR data (KBr pellet, cm^{-1}): 476 (w), 544 (m), 640 (s), 810 (m), 862 (w), 985 (m), 1022 (m), 1161 (m), 1224 (m), 1252 (m), 1384 (s), 1470 (s), 1633 (w), 2064 (vs, N_3), 2931 (m), 3376 (s, br).

*$[Mn^{III}_{12}Mn^{II}_6Cd^{II}(\mu_4\text{-}O)_8(\mu_3\text{-}Cl)_{1.2}(\mu_3\text{-}\eta^1\text{-}N_3)_{6.8}(HL^1)_{12}(MeCN)_6]Cl_{1.5}(CdCl_4)_{0.25}\cdot 14.5MeOH$ (**5**).* Complex **5** was prepared using the same procedure as for **3** but using $Cd(NO_3)_2\cdot 6H_2O$ (0.3 g, 0.97 mmol) in place of $Sr(NO_3)_2\cdot 6H_2O$. Black crystals of **5** were obtained after two days, washed with a small amount of MeCN, and dried in air over several days. Yield 19% (based on Mn). Elemental analysis (%) calcd for $C_{124}H_{158}Cd_{1.25}Cl_{3.7}Mn_{18}N_{26.4}O_{50}$ (**5**·4MeOH·2H_2O): C 34.61; H 3.69; N 8.59; found: C 34.71; H 3.45; N 8.48. Selected IR data (KBr pellet, cm^{-1}): 419 (w), 474 (m), 516 (w), 558 (s), 635 (vs), 659 (s), 768 (w), 812 (m), 864 (m), 901 (vw), 954 (w), 985 (m), 1026 (m), 1161 (m), 1224 (m), 1253 (s), 1320 (m), 1384 (m), 1470 (vs), 1615 (m), 2063 (vs, N_3), 2831 (m), 2864 (m), 2917 (m), 3001 (m), 3375 (s, br).

*$[Mn^{III}_{12}Mn^{II}_6Lu^{III}(\mu_4\text{-}O)_8(\mu_3\text{-}Cl)_{1.5}(\mu_3\text{-}\eta^1\text{-}N_3)_{6.5}(HL^2)_{12}(MeCN)_6]Cl_3\cdot 3H_2O\cdot 7MeOH\cdot MeCN$ (**6**).* A slurry of $NaO_2CMe\cdot 3H_2O$ (0.028 g, 0.2 mmol), NaN_3 (0.02 g, 0.3 mmol), $MnCl_2\cdot 4H_2O$ (0.04 g, 2 mmol), and 2,6-bis(hydroxymethyl)-4-fluorophenol (0.18 g, 1.05 mmol) in 15 mL of MeCN and 3 mL of MeOH was stirred for 30 min at room temperature; then, solid $Lu(NO_3)_3\cdot 6H_2O$ (0.047 g, 0.1 mmol) was added in small portions. The resulting mixture was stirred for additional 1 h and then heated at reflux for 2 h to afford a dark brown solution, which was cooled and filtered. Dark brown crystals of **6** were obtained after a few days. Yield: 16%. Elemental analysis (%) calc. for $C_{108}H_{114}Cl_{4.5}F_{12}LuMn_{18}N_{25.5}O_{50}$ (**3**·6H_2O): C 31.48; H 2.79; N 8.67; found: C 31.55; H 3.06; N 8.63. Selected IR data (KBr pellet, cm^{-1}): 474 (m), 550 (m), 640 (s), 812 (m), 864 (w), 984 (m), 1026 (m), 1161 (m), 1224 (m), 1252 (m), 1386 (s), 1470 (s), 1633 (w), 2062 (vs, N_3), 2931 (m), 3370 (s, br).

X-ray Data Collection and Structure Refinement. Data were collected at 100 K on a Bruker SMART Apex diffractometer (**3**−**5**) using a Mo Kα rotating-anode source. Data for **6** were measured at 150 K on the SCD beamline at the ANKA synchrotron, Karlsruhe, using a Bruker SMART Apex diffractometer and silicon-monochromated radiation with $\lambda = 0.8000$ Å (15.510 keV); f' and f'' for this wavelength were obtained by the method of Brennan and Cowan[19] as implemented on http://skuld.bmsc.washington.edu/scatter/AS_periodic.html. Data were corrected for absorption.[20a] Structure solution by direct methods and full-matrix least-squares refinement against F^2 (all data) were carried out using the SHELXTL package.[20b] All ordered non-H atoms were refined anisotropically. Some of the face-bridging ligands in **3**, **5**, and **6** were disordered superpositions of chloride and azide; refinement with appropriate restraints applied to azide geometries and to the temperature factors of closely separated chlorine and nitrogen atoms was straightforward. The relative occupancies of the azide and chloride ligands were adjusted to be consistent with the corresponding microanalytical data.

The two or three counteranions (nitrate for **4**, chloride for the others) accept hydrogen bonds from O(5)−H(5) and O(8)−H(8) and their symmetry equivalents; they are therefore disordered (against lattice MeOH) over twelve sites per $Mn_{18}M$ cluster. Refinement with appropriate partial occupancy Cl, O, and C atoms, and restraints on the C−O bond lengths, was straightforward. The hydrogen-bonded (half-occupancy) oxygen of the nitrate anion in **4** could be refined anisotropically, but the remaining atoms of the anion were probably further disordered, with significantly higher isotropic temperature factors. In the structure of **5**, most of the charge balance was provided by chloride anions, as described above, but a $[CdCl_4]^{2-}$ anion, twofold disordered over a site of $\bar{3}$ symmetry could be identified in the lattice. This could be refined with an overall occupancy of 25% per $Mn_{18}Cd$ cluster using anisotropic temperature factors, with a total of 1.5 chlorides per $Mn_{18}Cd$ for charge balance. The 75% of cavities that do not contain a tetrachlorocadmate presumably contain lattice

dx.doi.org/10.1021/ic3025588 | *Inorg. Chem.* 2013, 52, 5764−5774

Table 1. Crystallographic Data

	$Mn_{18}Sr$ (3)	$Mn_{18}Y$ (4)	$Mn_{18}Cd$ (5)	$Mn_{18}Lu$ (6)
formula	$C_{135}H_{198}Cl_{2.5}Mn_{18}N_{28.5}O_{59}Sr$	$C_{131}H_{182}Mn_{18}N_{33}O_{64}Y$	$C_{134.5}H_{196}Cd_{1.25}Cl_{3.7}Mn_{18}N_{26.4}O_{58.5}$	$C_{120}H_{145}Cl_{4.5}F_{12}LuMn_{18}N_{26.5}O_{54}$
Mr	4329.38	4320.93	4379.36	4331.96
crystal system	trigonal	trigonal	trigonal	trigonal
space group	$R\bar{3}$	$R\bar{3}$	$R\bar{3}$	$R\bar{3}$
T [K]	100(2)	100(2)	100(2)	150(2)
a [Å]	20.8150(16)	20.9556(10)	20.8765(12)	20.7696(13)
c [Å]	35.285(5)	34.328(2)	34.568(4)	33.081(2)
V [Å^3]	13240(2)	13055.2(12)	13047.3(18)	12358.6(13)
Z	3	3	3	3
ρ_{calcd} [g/cm^{-3}]	1.629	1.649	1.672	1.762
λ [Å]	0.71073	0.71073	0.71073	0.80000
μ [mm^{-1}]	1.663	1.678	1.550	2.821
$F(000)$	6630	6600	6686	6498
reflections collected	12 245	16 928	17 287	27 010
unique data	5179	5333	5915	5520
R_{int}	0.0599	0.0618	0.0646	0.0464
data with $[I > 2\sigma(I)]$	2959	3190	3461	4447
parameters/restraints	354/18	397/40	382/10	389/21
S on F^2 (all data)	0.977	1.011	1.006	1.048
wR_2 (all data)	0.2221	0.1650	0.1641	0.1705
R_1 $(I > 2\sigma(I))$	0.0739	0.0604	0.0508	0.0496
largest residuals [e Å^{-3}]	+2.06/−0.60	+0.76/−0.36	+1.02/−0.74	+3.25/−0.85
CCDC number	866694	866695	866696	866697

methanols, but these could not be located underneath the disordered electron-rich anion. To estimate the number of methanol molecules, SQUEEZE[21] was implemented on a structure from which the tetrachlorocadmate had been deleted, and 105 electrons per cavity (or per $Mn_{18}Cd$) were detected, compared to 104 e for $^1/_4[CdCl_4]^{2-}$ + 4MeOH. These were therefore added to the 10.5 methanols disordered against the chlorides, to estimate an approximate overall formulation with ca. 14.5 methanols per $Mn_{18}Cd$ complex.

For the structure of **4**, any attempts to refine these outer Mn^{II} sites as a Mn^{II}/Y^{III} mixture resulted in relative occupancies corresponding to pure Mn^{II}. In the remaining compounds, the heterometal is much heavier than Mn, and any "contamination" of the outer vertices with **M** would have been immediately obvious from the temperature factors. For the lanthanides, seven-coordination is highly unlikely.

Disordered lattice solvent molecules and counterions which could not be refined satisfactorily using partial atom occupancies and suitable restraints were handled using the SQUEEZE option in PLATON.[21] Crystallographic data and structure refinement details for compounds **3**–**6** are summarized in Table 1. Crystallographic data (excluding structure factors) for the structures in this paper have been deposited with the Cambridge Crystallographic Data Centre as supplementary publication nos. CCDC 866694–866697. Copies of the data can be obtained, free of charge, on application to CCDC, 12 Union Road, Cambridge CB2 1EZ, UK: http://www.ccdc.cam.ac.uk/cgi-bin/catreq.cgi; e-mail: data_request@ccdc.cam.ac.uk; or fax: +44 1223 336033.

Magnetic Measurements. Magnetic susceptibility measurements were obtained using a Quantum Design SQUID magnetometer MPMS-XL over the temperature range of 1.8–300 K, first using a dc field of 1000 Oe and, then, in zero dc field with an oscillating ac field of 3 Oe and ac frequencies of 100 or 200 Hz. Magnetization measurements were made over a range of temperatures of 1.8–300 K with dc applied fields from 0 to 7 T. Measurements were performed on fresh, still solvent-containing polycrystalline samples. The measurements of M versus H at 100 K were additionally used to check for the presence of ferromagnetic impurities, which were found to be absent. All measurements were performed on freshly filtered crystalline samples (to minimize lattice solvent loss) which were finely ground and restrained in grease, and magnetic data were corrected for the sample holder and the diamagnetic contribution which was calculated from Pascal's constants.[22]

Computational Methods. The computer code employed for the all calculations was the program SIESTA[23−25] (Spanish Initiative for Electronic Simulations with Thousands of Atoms). We employed the generalized-gradient functional proposed by Perdew, Burke, and Erzernhof[26] using the DFT+U option[27] with a U value of 4.0 eV. The results for the weak central intertetrahedron interaction using the PBE functional do not give an agreement with the experimental data that it is obtained using the PBE+U modification. Only valence electrons are included in the calculations, with the core being replaced by norm-conserving scalar relativistic pseudopotentials factorized in the Kleinman-Bylander form.[28] The pseudopotentials are generated according to the procedure of Trouiller and Martins.[29] For the Mn atoms, we used a pseudopotential including the 3s and 3p orbital in the basis set that we have previously tested to give accurate J values.[30] In addition, a numerical basis set of triple-ζ quality with polarization functions for the manganese atoms and a double-ζ one with polarization functions for the main group elements were used. Previously, we have studied the influence of two main parameters of the Siesta code, the energy shift and the mesh cutoff, on the calculated J value for 3d systems.[31] Thus, the values of 50 meV for the energy shift and 250 Ry for mesh cutoff provide a good compromise between accuracy and computer time to estimate exchange coupling constants. The crystal structures were directly employed for the calculations considering the presence of eight azido ligands coordinated to the Mn^{III} cations. The calculated J values were obtained using a nonspin projected approach[32−35] and the following spin Hamiltonian:

$$\hat{H} = -\sum_{i>j} 2J_{ij}\hat{S}_i\hat{S}_j \quad (1)$$

For the $[Mn_{18}\mathbf{M}]$ complexes, eleven spin distributions were calculated to fit a system of ten equations with the eight or nine unknown J values: the high spin $S = 78/2$ distribution, an $S = 0$ configuration with the inversion of the spins of one of the Mn_9 moieties, and eight distributions with the following total spin and metal atoms with negative spins (see Figure 5): $S = 62/2$ {Mn7, Mn11}, $S = 62/2$ {Mn1, Mn4}, $S = 52/2$ {Mn1, Mn6, Mn16}, $S = 46/2$ {Mn3, Mn4, Mn7, Mn11}, $S = 34/2$ {Mn2, Mn5, Mn6, Mn15, Mn17}, $S = 30/2$ {Mn1,

dx.doi.org/10.1021/ic3025588 | Inorg. Chem. 2013, 52, 5764−5774

Mn2, Mn3, Mn4, Mn5, Mn6}, S = 30/2 {Mn7, Mn8, Mn9, Mn10, Mn11, Mn12 }, S = 26/2 {Mn1, Mn5, Mn9, Mn10, Mn14, Mn18}, and S = 18/2 {Mn13, Mn14, Mn15, Mn16, Mn17, Mn18}.

RESULTS AND DISCUSSION

Synthesis. Previously, we communicated the syntheses, structures, and magnetic properties of the [Mn_{19}] aggregate (**1**)[4] and the heterometallic SMM [$Mn_{18}Dy$] (**2**).[12] Compound **2** was obtained through the targeted replacement of the central Mn^{II} in **1** with the highly anisotropic lanthanide ion Dy^{3+}, which could be achieved by the simple addition of $Dy(NO_3)_3{\cdot}6H_2O$ to the reaction mixture. In contrast, attempts to react **1** directly with the appropriate Dy^{3+} salts failed to yield **2**. We have now extended the successful methodology that yielded **2**, showing that simple addition of Sr^{2+}, Y^{3+}, Cd^{2+}, and Lu^{3+} salts to the synthetic reaction for **1** results in the synthesis of compounds **3**−**6**, respectively, in good yield. It should be noted that various Mn/**M** ratios were explored, but the best results were obtained with the stoichiometry reported here. Initial attempts to obtain a $Mn_{18}Lu$ complex using the ligand H_3L^1 were unsuccessful; no crystalline product was obtained. However, using the related ligand H_3L^2, in which the methyl substituent on the phenol ring is replaced by a fluorine atom, complex **6** was obtained in appreciable yield.

The IR spectra of all the compounds exhibit very strong absorption bands at 2059−2076 cm^{-1} corresponding to the azido asymmetric vibrations.[36] In compound **1**, all the face-bridging ligands were azides,[4] while in **2** a disordered mixture of azides and chlorides was found.[12] This was also the case for compounds **3**, **5**, and **6**, although the chlorides are in a small minority. The $Mn_{18}Y$ compound **4** could be obtained from a reaction in which only nitrate salts of the two metals were used, so that chloride ions were completely absent and the resulting complex only contains azides. Unfortunately, using this synthetic approach did not give single crystals with the other heterometals. However, DFT calculations on **1** have already suggested that, although the end-on azides play some role in mediating the Mn^{III}−Mn^{III} ferromagnetic interactions within this and similar compounds, it is the $(\mu_4\text{-O})^{2-}$ ligands which provide the dominant pathway for the ferromagnetic interactions, and replacement of azides by other face-bridging μ_3-ligands was not expected to have a significant effect on the magnetic interactions.[11]

A clean replacement of the central Mn^{II} in **1** by the diamagnetic heterometal cation to give the respective [Mn_{18}**M**] species (**3**−**6**) was observed. The diamagnetic heterometal ions used here have a much stronger preference for eight-coordinate environments and so select the eight-coordinate central position. As was found for **1** and **2**, the chloride counterions accept hydrogen bonds from the alcohol −OH groups of the organic ligands and are disordered against lattice methanols. Interestingly, in compound **5**, the counterions were found to be a mixture of both chloride and a small proportion of the tetrachlorocadmate dianion.

Description of Structures. Compounds **3**−**6** all crystallize in the same trigonal space group $R\bar{3}$ with Z = 3 and are also all isomorphous to the previously reported {Mn_{19}} complex **1** and the {$Mn_{18}Dy$} complex **2**.[4,12] Compounds **1**−**6** are closely isostructural, with crystallographic −3 site symmetry, mainly differing (apart from the heterometal) in the relative number of face-bridging azide and chloride ligands, so the structure of **3** (see Figure 2a) will be described here as an example. The core of **3** can be considered as consisting of two supertetrahedral

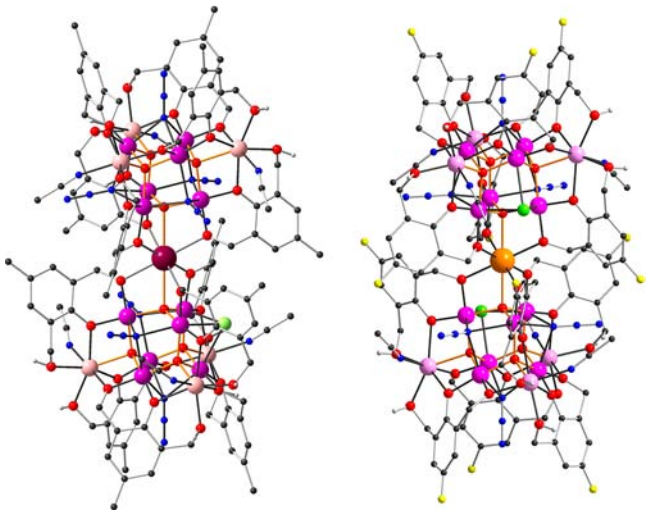

Figure 2. Molecular structures of **3** and **6** in the crystal. Organic H atoms, counterions, and lattice solvent molecules have been omitted for clarity. In each case, only one of the possible distributions of disordered azide and chloride ligands is shown. Color code: Mn^{III}, purple; Mn^{II}, pink; Sr, crimson; Lu, orange; Cl, green; F, yellow; O, red; N, blue; C, dark gray.

{$Mn^{III}_6Mn^{II}_3Sr$} units sharing a common Sr vertex. Four of the faces of the central Mn^{III}_6 octahedron in each supertetrahedron are bridged by oxo ligands, which each further coordinate to a Mn^{II} vertex, forming $(\mu_4\text{-O})^{2-}$ bridges. The remaining four Mn^{III}_3 triangles of the superterahedron are bridged by face-bridging μ_3-ligands; there are thus eight such ligands per cluster. In **3**, the two such ligand sites, which lie on the crystallographic 3-fold axis and are thus opposite to Sr(1), are occupied by azides. The remaining six (crystallographically equivalent) sites appeared initially also to be occupied by azides; however, residual electron density between the coordinated and central nitrogens was consistent with a small proportion of these sites being occupied by chloride ligands. This was consistent with the microanalytical data; the N/C ratio was rather low for an all azide model, and the data fitted better to a formulation with an average composition of 7.5 azides and 0.5 chloride per $Mn_{18}Sr$ cluster. The relative site occupancies were then fixed to be consistent with this formulation in the final refinement. The Mn−Cl distances for the minor chloride component were consistent with those found in **2**.[10] Such mixtures of azide/chloride face-bridging ligands were also observed in compounds **5** and **6**. Of the compounds reported here, only **4**, for which the synthetic reaction mixture contained no chlorides, has all eight such ligands as azides, as was also the case for **1**.[4]

Each supertetrahedral edge is bridged by an organic $(HL^1)^{2-}$ ligand. As in **1** and **2**, the two deprotonated oxygens each bridge between two metal centers, with the remaining $-CH_2OH$ group coordinating to an outer Mn^{II} center, Mn(3). The organic ligands $(HL^2)^{2-}$ in **6** have a fluoro substituent at the *para*-position on the phenol ring in place of the methyl group in the $(HL^1)^{2-}$ ligands of the other compounds. The coordination is the same as seen for the $(HL^1)^{2-}$ ligands, although the temperature factors for the fluorine atoms and the adjacent carbons on the rings are rather anisotropic, suggesting that the smaller fluorine atom does not fit quite as snugly in the crystal structure as the larger methyl group.

dx.doi.org/10.1021/ic3025588 | Inorg. Chem. 2013, 52, 5764−5774

In the structures of **3**–**6**, it was clear that only the central metal center had been replaced by the heterometal ion. Sr, Y, Cd, and Lu ions all have significantly higher X-ray scattering factors than Mn, and there was no indication from the structure refinements to suggest anything other than pure heterometal at the central position with no detectable substitution of Mn^{II} at the outer seven-coordinate sites. In the original structure of **1**, the temperature factors of the four independent Mn centers were very similar, being slightly lower for the Mn^{III} than the Mn^{II} sites: U_{eq} taking the values of 0.0251(2), 0.02156(12), 0.02127(12), and 0.02446(12) $Å^2$ for Mn(1), Mn(2), Mn(3), and Mn(4), respectively.[4] Very similar patterns were found for the corresponding metal centers in **3**–**6** and also in **2**,[12] which makes good chemical sense in that these metal ions are all commonly found with coordination number eight, with seven-coordination being less common and with the opposite being true for Mn^{II}.

Since the main difference between the structures of compounds **3**–**6** is the replacement of the central metal site, the geometries of the linkages between the two Mn_9 units needs to be examined. The geometries (bond lengths and angles) involving the oxo ligand O(1) and the alkoxo bridge O(4), Figure 3, are summarized in Table 2, where they are also

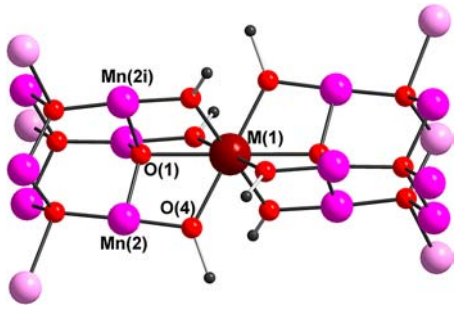

Figure 3. Bridges involving O(1) and O(4) in compounds **1**–**6**.

compared with the corresponding data for **1** and **2**.[4,12] The geometries within this part of the structure are already known to be critical for the molecular magnetic properties. In the Mn_{19} analogue reported by Kou et al., in which the MeCN ligands of **1** have been replaced by H_2O, an increase in the Mn(2)–O(1)–Mn(1) bond angle from 101.79(8)° in **1** to 102.4(2)° appears to have been largely responsible (the Mn(1)–O(1) distance does not differ significantly between the two compounds) for switching the Mn(2)···Mn(1) interaction from ferromagnetic to antiferromagnetic, resulting in a reduced spin ground state of $S = 73/2$.[4,5,11]

An examination of the data presented in Table 2 underlines the closely isostructural nature of these compounds. This is an important feature in terms of the subsequent magnetic and theoretical studies, where we wish to determine the ability of the diamagnetic central ion to transmit magnetic information between the two $S = 39/2$ $\{Mn^{II}_3Mn^{III}_6\}$ subunits. If we are to speculate on electronic structural rationalizations of any superexchange, then it is necessary to keep all other parameters as fixed as possible.

Comparing the geometries about O(1), there is a clear distinction between the complexes with a divalent central metal ion and those with a trivalent M(1). In **2**, **4**, and **6**, the M(1)–O(1) distances (2.438–2.452 Å) are, as expected, consistently shorter than those in **1**, **3**, and **5** (2.509–2.661 Å), even allowing for the differing ionic radii of the central ion M(1). The electronic configurations and the ionic radii for 8-coordinate M^{2+} and M^{3+} cations are given in Table 3. The

Table 3. Electronic Configurations and Ionic Radii[37] for the 8-Coordinate M(II) and M(III) Cations in Compounds 1 and 3–6 and for the Ions Used in Calculations (See Text)

cation	electronic configuration	Ionic radius (VIII coordination)
Mn^{2+}	[Ar] $3d^5$	0.96 (0.90 for VII coordination)
Rb^+	[Kr] ≡ [Ar] $4s^2$ $3d^{10}$ $4p^6$	1.56
Sr^{2+}	[Kr] ≡ [Ar] $4s^2$ $3d^{10}$ $4p^6$	1.26
Y^{3+}	[Kr] ≡ [Ar] $4s^2$ $3d^{10}$ $4p^6$	1.02
Zr^{4+}	[Kr] ≡ [Ar] $4s^2$ $3d^{10}$ $4p^6$	0.84
Ba^{2+}	[Xe] ≡ [Kr] $5s^2$ $4d^{10}$ $5p^6$	1.42
Cd^{2+}	[Kr] $4d^{10}$	1.10
In^{3+}	[Kr] $4d^{10}$	0.98
Hg^{2+}	[Xe] $4f^{14}$ $5d^{10}$	1.14
Lu^{3+}	[Xe] $4f^{14}$	0.98

Mn(2)–O(1) distances show the opposite trend, being shorter when M(1) is divalent than when it is trivalent, 1.883–1.910 Å compared to 1.915–1.929 Å. This affects the angles about O(1), and the Mn(2)–O(1)–M(1) angles are larger for trivalent M(1) (103.0–103.5°) than for divalent M(1) (101.6–102.2°) with correspondingly opposite but smaller differences for the Mn(2)–O(1)–Mn(2^i) angles.

Magnetic studies. The magnetic properties of the $[Mn_{18}M]$ (**M** = Sr, **3**; Y, **4**; Cd **5**; Lu, **6**) compounds were measured on polycrystalline samples. The susceptibility and magnetization data for **3**–**6** are summarized in Table 4 and shown in Figure 4. For compounds **3**–**6**, the ac susceptibility was checked but showed no out-of-phase signal above 1.8 K and no frequency dependence of the in-phase component.

The χT products for compounds **3**–**6** at 300 K are all significantly higher than the expected value for twelve

Table 2. Selected Bond Lengths (Å) and Angles (°) Involving the Bridging Oxygens O(1) and O(4) in the $[Mn_{19}]$ and $[Mn_{18}M]$ Systems

	$Mn_{18}Mn^{II}$ (**1**)	$Mn_{18}Dy^{III}$ (**2**)	$Mn_{18}Sr^{II}$ (**3**)	$Mn_{18}Y^{III}$ (**4**)	$Mn_{18}Cd^{II}$ (**5**)	$Mn_{18}Lu^{III}$ (**6**)
Mn(2)–O(1)	1.8907(7)	1.929(2)	1.9105(17)	1.9148(16)	1.8826(14)	1.9153(13)
O(1)–M(1)	2.509(3)	2.440(9)	2.658(7)	2.452(6)	2.542(6)	2.437(5)
Mn(2)–O(1)–M(1)	101.79(8)	103.0(3)	102.3(2)	103.49(17)	101.58(18)	103.38(14)
Mn(2)–O(1)–Mn(2^i)	115.93(5)	115.1(2)	115.59(14)	114.73(13)	116.07(12)	114.82(11)
Mn(2)–O(4)	1.8545(18)	1.848(6)	1.861(4)	1.872(4)	1.842(4)	1.869(3)
Mn(2)–O(4)–M(1)	109.29(8)	109.4(2)	108.47(19)	108.12(16)	108.81(15)	109.13(13)
O(4)–M(1)	2.3447(17)	2.345(5)	2.535(4)	2.367(4)	2.387(3)	2.328(3)
	ref 4	ref 12	this work	this work	this work	this work

dx.doi.org/10.1021/ic3025588 | *Inorg. Chem.* 2013, 52, 5764–5774

Table 4. Susceptibility and Magnetization Data for Compounds 3−6

compounds	χT at 1.8 K (cm^3K/mol)[a]	maximum value of χT (cm^3K/mol)[a]	T for maximum in χT curve	χT at 300 K (cm^3K/mol)[a]	M at 1.8 K, 7 kOe (μ_B)	J'/k_B (K)[b]
Mn_{19} (**1**)[4]	894			93	84.5	0
$Mn_{18}Sr$ (**3**)	140.4	360.4	18	88.6	80.5	−0.0025
$Mn_{18}Y$ (**4**)	77.3	296.6	22	77.2	68.8	−0.0058
$Mn_{18}Cd$ (**5**)	555.7			82.9	80.0	0
$Mn_{18}Lu$ (**6**)	74.5	282.4	24	78.3	69.5	−0.0067

[a]Zero dc field with ac field of 3 Oe at 100 Hz (Y) or 200 Hz (Sr, Cd, Lu). [b]Coupling between the two Mn_9 subunits, from equalizing the exchange and the Zeeman terms (see text).

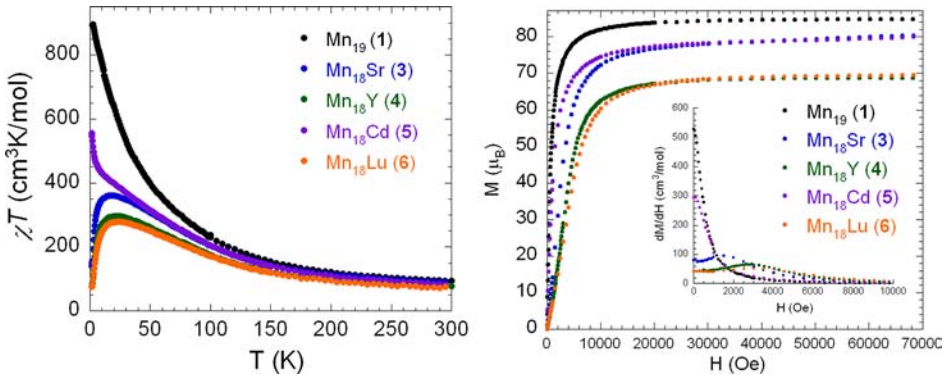

Figure 4. (Left) Temperature dependence of the χT products of **1** and **3−6** (where $\chi = dM/dH$) measured in H_{dc} = 0 Oe, H_{ac} = 3 Oe, and ν = 100 or 200 Hz. (Right) Field dependence of the magnetization of **1** and **3−6** at 1.8 K; inset: derivative plots of dM/dH vs H at 1.8 K.

noninteracting S = 2 Mn^{III} and six S = 5/2 Mn^{II} ions (62.25 cm^3K/mol taking g_{av} = 2). This is similar to what was observed for the parent Mn_{19} compound **1** and indicates that once again ferromagnetic interactions dominate within these compounds and the respective χT products increase as the temperature decreases.

The [$Mn_{18}Cd$] compound **5** shows very similar behavior to the parent compound **1** over the full temperature range. If the susceptibility is measured using a small ac applied field of 3 Oe oscillating at 200 Hz, χT increases steadily to reach a value of 555.7 cm^3K/mol at 1.8 K. As was the case for **1**, the use of even a very small dc applied field results in a downturn of χT at low temperatures due to saturation effects. The magnetization data for **5** also show a behavior very similar to that for **1**, with an initial very rapid rise in M with no detectable inflection point, followed by complete saturation. The saturation value of 80.0 μ_B is in good agreement with the expected value of 78 μ_B (assuming g_{av} = 2) for two noninteracting Mn_9 units each with a spin S_T = 39/2 ground state. In fact, the reduced magnetization data (M vs H/T) below 20 K superpose on a master curve and can be fitted almost perfectly using the sum of two Brillouin functions for S_T = 39/2 spins with g = 2.02 (Figure S1, Supporting Information). In summary, the Mn_9 subunits in **5** show negligible anisotropy with a well-defined spin ground state, and there is no evidence for any antiferromagnetic interaction between the two Mn_9 subunits. We cannot, of course, rule out a weak *ferro*magnetic interaction from the data available.

Compounds **3**, **4**, and **6**, in contrast, show different behavior. Although, as for **1** and **5**, they all show a similar increase in χT as the temperature is lowered; this now reaches a maximum at ca. 20 K, followed by a rapid decrease on further lowering the temperature to 1.8 K. This behavior is still observable even when switching off the dc field and using an oscillating ac field. Such a downturn might normally be attributed to either intermolecular interactions or zero-field splitting effects at the Mn^{III} centers. However, neither explanation is valid here. First, compounds **3−6** all crystallize isomorphously with the Mn_{19} complex **1** and any intermolecular interactions in **3**, **4**, and **6** should therefore also be present in **1** and **5**, but no such downturn was observed for these two compounds. Second, the geometries about the Mn^{III} centers in all these five compounds are very similar; so if ZFS effects are visible in **3**, **4**, and **6**, they should also be observable in **1** and **5**, but they are not. The downturn in χT for **3**, **4**, and **6** must therefore be assigned to weak antiferromagnetic interactions between the Mn_9 subunits mediated by the central **M** cations. The presence of these antiferromagnetic interactions is supported by the M vs H plots at low fields in which inflection points can be observed, and the positions of these, at H = 1480 (**3**), 2850 (**4**), and 3290 (**6**) Oe, can be seen more clearly from the maxima on the dM/dH vs H plots (Figure 4 right, inset). For the $Mn_{19}Sr$ compound **3**, assuming that only the S_T = 39/2 ground state is populated below 4 K for each of the Mn_9 units, the exchange interaction can be estimated by equalizing the exchange and the Zeeman terms: $8|J|S_{T1}S_{T2} = 2g\mu_B HS_T$ implying that $J/k_B \approx -0.0025$ K. Due to the presence of this inter-Mn_9 interaction, it is not possible to obtain a good fit to a Brillouin function below 4 K. Moreover, the presence of excited states also precludes considering data above 10 K, and so we have restricted the Brillouin fitting to consider only the data from 4 to 10 K. Plotting the data for the [$Mn_{18}Sr$] compound **3** between 4 and 10 K as reduced magnetization M vs H/T shows that the data are all superposed on to one single master curve, indicating that in this temperature range the Mn_9 subunits have only their ground states thermally populated and that the weak antiferromagnetic interaction between them is suppressed by thermal fluctuations. Consistent with this, the M vs H/T plots can be well fitted by the sum of two Brillouin functions, each for a S_T = 39/2 spin with g = 2.01 (Figure S2, Supporting

dx.doi.org/10.1021/ic3025588 | Inorg. Chem. 2013, 52, 5764−5774

Information). This result confirms the S_T = 39/2 ground state for the Mn_9 units.

However, although the magnetization data for **3** and **5** are in good agreement with two Mn_9 units each with S = 39/2, either isolated as for **5** or with very weak antiferromagnetic coupling between them as for **3**, the corresponding data for the $[Mn_{18}Y]$ compound **4** and $[Mn_{18}Lu]$ compound **6** cannot be analyzed so simply. The magnetization for each of these only reaches a saturation value of ca. 70 μ_B at 7 T and 1.8 K, well below the values for the other two compounds, suggesting that the Mn_9 units in **4** and **6** have a spin ground state that is lower than the fully ferromagnetic S_T = 39/2 and more in line with S_T = 33/2 or 35/2. The reduced magnetization data for **4** between 7 and 15 K, with the temperature range again chosen to remove the influences of both inter-Mn_9 coupling and excited states, could be fitted to the sum of two Brillouin functions for S_T = 33/2, 35/2, 37/2, or 39/2 spins, giving g-values of 2.05, 1.94, 1.83, or 1.74, respectively (Figure S3, Supporting Information). The reduced magnetization data for **6** between 4 and 10 K could likewise be fitted to the sum of two Brillouin functions for either S_T = 33/2 or 35/2 spins, giving respective g-values of 2.07 and 2.00 (Figure S4, Supporting Information). Given that the magnetization of the parent Mn_{19} compound **1** was fitted with a Brillouin function for S = 83/2 and g = 2.00(6),[4] then the most likely spin ground state for each Mn_9 unit in compounds **4** and **6** corresponds to either S_T = 33/2 or 35/2. If we compare the maximum values for $\chi'T$ (296 cm^3K/mol at 22 K for **4**; 282 cm^3K/mol at 24 K for **6**) with the expected values for either two S_T = 33/2 units or for two S_T = 35/2 units (with g = 2) which are 289 or 324 cm^3K/mol, respectively, then the S_T = 33/2 state clearly gives better agreement. Taking this value and equalizing the exchange and the Zeeman terms as before using $8|J|S_{T1}S_{T2} = 2g\mu_B HS_T$, the inter-$Mn_9$ exchange interactions can be estimated as $J/k_B \approx -0.0058$ K for **4** and $J/k_B \approx -0.0067$ K for **6**, respectively.

The reason for the lower spin states within the Mn_9 units in **4** and **6** (a reduction from S = 39/2 to S = 33/2) is not obvious. Clearly, they could arise simply from questions concerning the formula weights used or sample quantities. However, if these lower spin states were merely experimental artifacts, rather than something intrinsic to the molecules, it would then be an extreme coincidence that such a problem was identical in magnitude for the two compounds involved. We therefore believe that these lower spin states are intrinsic to these two molecules and must have something to do with the nature of the central M^{III} ion. Although the origin of this behavior is most likely to be found within the central Mn^{III}_3··M^{III}··Mn^{III}_3 units, with the evidence currently on hand, it would be unwise to speculate further.

DFT Calculations. The synthesis and isolation of $[Mn_{18}\mathbf{M}]$ complexes (**M** = Sr, **3**; Y, **4**; Cd **5**; Lu, **6**) provided a good opportunity to examine the nature of the magnetic interaction between the $\{Mn^{II}_3Mn^{III}_6\}$ units in the $[Mn_{19}]$ system through these closed shell metal ions which differ in the energies and nature of their valence orbitals. To provide further insight into the experimental results, we carried out density functional calculations of these four $[Mn_{18}\mathbf{M}]$ systems together with the original Mn_{19} one using the Siesta code with a numerical basis set and the PBE+U functional, U = 4.0 eV, (see Computational Methods section). The topology of the exchange coupling constants in such systems is described in Figure 5, and the results are collected in Table 5.

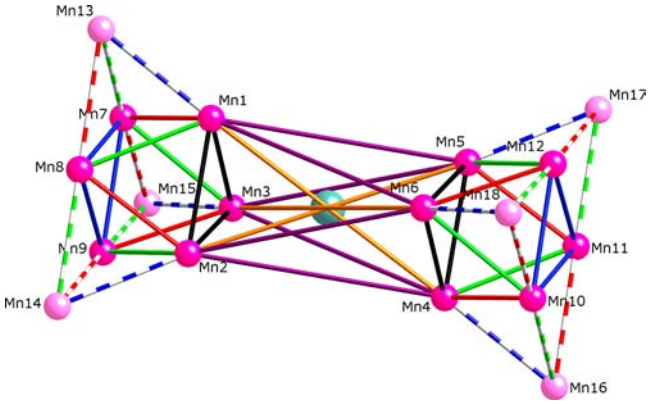

Figure 5. Topology of the exchange coupling constants for the $Mn_{18}\mathbf{M}$ systems, J_1–J_4 solid lines (black, red, green, and blue, respectively) corresponding to Mn^{III}···Mn^{III} coupling through μ_4-O and μ_3-N_3 bridging ligands and J_5–J_7 dashed lines (blue, green, and red, respectively) of Mn^{III}···Mn^{II} couplings through μ_4-O and μ-OR bridging ligands. The nine inter-Mn_9 interactions are indicated with violet and orange solid lines averaged in the J_8 value.

The analysis of the results in Table 5 leads to the following conclusions: (i) All the intra-Mn_9 tetrahedron exchange interactions are ferromagnetic. (ii) The J_1–J_4 values (Mn^{III}···Mn^{III} interactions) for the four $Mn_{18}\mathbf{M}$ complexes are larger than those of the original Mn_{19} one while the J_5–J_7 constants (Mn^{III}···Mn^{II} interactions) are very similar. (iii) The calculated inter-Mn_9 interactions, −0.003, −0.005 and −0.007 K, reproduce the experimental estimations extremely well (−0.0025, −0.0058 and −0.0067 K) for the $Mn_{18}Sr$(**3**), $Mn_{18}Y$(**4**) and $Mn_{18}Lu$(**6**) complexes, respectively. (iv) The unique experimental behavior of the $[Mn_{18}Cd]$ is theoretically reproduced with the calculated J value being negligible; thus unlike in the other $[Mn_{18}\mathbf{M}]$ complexes, there is no antiferromagnetic coupling between the Mn_9 supertetrahedrons. (v) From the theoretical point of view, the PBE+U J values are closer to those previously obtained with the PBE functional than the hybrid B3LYP results.[26] This behavior seems to be related to the ferromagnetic nature of the interaction while the opposite one is usual for antiferromagnetic couplings.

A question that arises from the previous results is the origin of the differences between the inter-Mn_9 interactions in the $[Mn_{18}\mathbf{M}]$ systems, i.e., whether they are due to structural differences or to the electronic configuration of the central diamagnetic metal. In order to clarify this point, calculations were performed by using the structure of the $[Mn_{18}Y]$ complex but replacing the central Y^{III} metal by the Lu^{III}, Sr^{II}, and Cd^{II} cations (see complete results in Table S1, Supporting Information). The calculated J_9 values are now −0.012, −0.005, −0.004, and +0.012 K, respectively, for the Lu^{III}, Y^{III}, Sr^{II}, and Cd^{II} systems. These values follow the same trend as those obtained with the original $[Mn_{18}\mathbf{M}]$ structures, clearly indicating that the different behavior is due to the electronic structure of the central cation. Cd^{2+}, with its outermost filled shell of 4d orbitals, seems to be genuinely "innocent", not mediating any significant interaction between the Mn_9 subunits, and Sr^{2+}, Y^{3+}, and Lu^{3+}, however, with their outermost electrons in (ns^2np^6) orbitals, are able to mediate weak antiferromagnetic interactions of magnitude $J/k_B \approx -0.002$ to −0.007 K. It is worth mentioning that this small structural change when using the $[Mn_{18}Y]$ structure in the calculation now results in a

dx.doi.org/10.1021/ic3025588 | Inorg. Chem. 2013, 52, 5764–5774

Table 5. Calculated J Values (in K) for the $Mn_{18}M$ Systems 3−6 and the Mn_{19} Complex 1 Using the Siesta Code and the PBE+U Functional[a]

	bridging ligand	$Mn_{18}Lu$ (6)	$Mn_{18}Cd$(5)	$Mn_{18}Y$ (4)	$Mn_{18}Sr$ (3)	Mn_{19} (1)
J_1	μ_4-O, μ_3-N_3	13.3	14.3	12.4	11.3	12.0 (11.8)
J_2	μ_4-O, μ_3-N_3	13.1	11.6	12.7	11.6	10.1 (8.9)
J_3	μ_4-O, μ_3-N_3	10.6	10.9	10.4	11.9	9.0 (8.4)
J_4	μ_4-O, μ_3-N_3	14.1	14.7	14.6	14.6	14.1 (15.4)
J_5	μ_4-O, μ-OR	7.3	7.0	7.0	7.7	7.4 (4.9)
J_6	μ_4-O, μ-OR	6.1	6.6	6.3	6.1	6.7 (4.0)
J_7	μ_4-O, μ-OR	6.9	6.0	6.6	6.9	7.0 (4.8)
J_8	O−M−O	−0.11	0.00	−0.07	−0.04	5.3[b] (2.5)
J_9	O−M−O	−0.007	0.000	−0.005	−0.003	

[a]Values in parentheses are those obtained using the PBE functional in ref 11. For the inter-Mn_9 interactions, two options were considered: an average J value of the eight interactions (see Figure 5), one assuming the local spins of the involved Mn^{III} cations (J_8) and the second one considering this interaction as two S = 39/2 interacting subsystems (J_9). [b]μ_4-O, μ-OR bridging ligands

ferromagnetic calculated J_9 value for the Cd^{II} complex; however, this is not particularly significant as this change in J_9 is no greater than that for the other systems, and it is only that the original J_9 was so close to zero that it has now switched to a positive value. For a given electron configuration, the main difference between the studied systems is the charge of the central cation. Thus, the systems containing trivalent cations show a stronger antiferromagnetic contribution for the intra-Mn_9 interactions than those with divalent cations.

With the aim of providing further insights into the role of central diamagnetic cation in the inter-Mn_9 exchange interactions, we performed calculations with some hypothetical nonsynthesized $[Mn_{18}\mathbf{M}]$ complexes by using again the $[Mn_{18}Y]$ structure to facilitate the comparison of the results. It should be borne in mind that such calculations allow us to obtain some qualitative indications, recognizing the limitations of using the $[Mn_{18}Y]$ structure for other cations. Thus, we have considered three new systems with ions isoelectronic to Y^{III} and Sr^{II}, viz., the Rb^{I}, Ba^{II}, and Zr^{IV} cations. The calculated J_9 values (see full set of J values in Table S1, Supporting Information) for these new cases are −0.009, −0.008, and −0.013 K, respectively. These results indicate that such cations always lead to an antiferromagnetic coupling between the Mn_9 moieties, but here, there is no clear relationship with the charge of the cations. To provide some results for comparison with the singular behavior of the $[Mn_{18}Cd]$ compound, which is the only case where J_9 is found to be zero, we studied two hypothetical complexes $[Mn_{18}Hg]$ and $[Mn_{18}In]$. Here, when the central cation is Hg^{II}, the electronic structure and charge is comparable to Cd^{II} but with the valence electrons in higher energy orbitals, and in the case of In^{III}, the ion is isoelectronic but the ion carries a higher positive charge. The calculated J_9 values (see full set of J values in Table S2, Supporting Information) are +0.024 and −0.009 K, respectively, so that J_9 for $Mn_{18}In$ is very weakly antiferromagnetic and close to the zero found for $[Mn_{18}Cd]$, while that for $[Mn_{18}Hg]$ is now weakly ferromagnetic. The difference between the values for divalent Hg^{II} and trivalent In^{III} is comparable to that found between $[Mn_{18}Sr]$ and $[Mn_{18}Y]$; however, now the two values happen to be on either side of zero. In any case, the calculations for the hypothetical $[Mn_{18}Hg]$ and $[Mn_{18}In]$ complexes confirm the unique behavior for Cd^{II} seen from the experimental data; these three central cations, having a very similar nd^{10} electronic configuration in the outermost shell, mediate either no or a very weakly ferromagnetic interaction between the Mn_9 subunits, in contrast to the metal ions with either a full rare gas configuration or with a full nf^{14} subshell as valence electrons.

CONCLUSIONS

The general synthetic route to the heterometallic $[Mn_{18}\mathbf{M}]$ structural type based on the targeted replacement of the central Mn^{II} in the original $[Mn_{19}]$-aggregate (**1**) with various heterometals, in analogy to the synthesis of $[Mn_{18}Dy]$ (**2**),[12] has been expanded to incorporate Sr (**3**), Y (**3**), Cd (**5**), and Lu (**6**). This successful synthesis opens a door to a family of $[Mn_{18}\mathbf{M}]$ complexes.

It is clear from the magnetic studies presented here that many diamagnetic metal cations are capable of mediating weak antiferromagnetic interactions between magnetic units, and when these subunits have a high spin, then the effects of this exchange become significant. However, not all such cations have this capability; Cd^{2+}, with its outermost filled shell of 4d orbitals seems to be genuinely "innocent" in this regard. Sr^{2+}, Y^{3+}, and Lu^{3+}, however, with their outermost electrons in (ns^2np^6) orbitals, are indeed able to mediate weak antiferromagnetic interactions of magnitude $J/k_B \approx -0.002$ to −0.007 K. Furthermore, the Y^{3+} and Lu^{3+} cations seems to be even less "innocent" than the others, in that, in addition to mediating these antiferromagnetic interactions, they also seem to have perturbed some of the Mn^{III} spins within the Mn_9 subunits in **4** and **6**. Clearly, the common use of Y^{3+} as a diamagnetic "honorary lanthanide ion" to replace paramagnetic lanthanides in the magnetic study of a series of isostructural 3d/4f coordination clusters should be carried out with perhaps a degree of caution. Further work is underway to test the scope and limitation of replacing the central Mn^{II} in **1** with a variety of heterometal cations to evaluate the magnetic contributions of such species within the $[Mn_{18}\mathbf{M}]$ system.

ASSOCIATED CONTENT

Supporting Information

CIF and additional structural data and magnetism figures. This material is available free of charge via the Internet at http://pubs.acs.org.

AUTHOR INFORMATION

Corresponding Author

*E-mail: annie.powell@kit.edu (A.K.P.); clerac@crpp-bordeaux.cnrs.fr (R.C.); eliseo.ruiz@qi.ub.es (E.R.); manase.ayuk@kit.edu (A.M.A.). Fax: +49-721-608-48142 (A.K.P.); +33 5 56 84 56 00 (R.C.); +34 93 4907725 (E.R.); +49 721

60848142 (A.M.A.). Tel: +49-721-608-42135 (A.K.P.); +33 5 56 84 56 50 (R.C.); +34 93 4037058 (E.R.); +49 721 60843485 (A.M.A.).

Notes

The authors declare no competing financial interest.

■ ACKNOWLEDGMENTS

This work was supported by DFG (CFN and SPP 1137), MagMaNet (NMP3-CT-2005-515767), Conseil Régional d'Aquitaine, Université de Bordeaux, CNRS, *Ministerio de Ciencia e Innovación* (CTQ2008-06670-C02-01), and *Generalitat de Catalunya* (2009SGR-1459). The authors thankfully acknowledge the computer resources, technical expertise, and assistance provided by the Barcelona Supercomputer Center. S.G.C. thanks the Spanish Ministerio de Educación, Cultura y Deporte for a predoctoral fellowship.

■ REFERENCES

(1) (a) Ferreira, K. N.; Iverson, T. M.; Maghlaoui, K.; Barber, J.; Iwata, S. *Science* **2004**, *303*, 1831. (b) Carrell, T. G.; Tyryshkin, A. M.; Dismukes, G. C. *J. Biol. Inorg. Chem.* **2002**, *7*, 2. (c) Cinco, R. M.; Rompel, A.; Visser, H.; Aromi, G.; Christou, G.; Sauer, K.; Klein, M. P.; Yachandra, V. K. *Inorg. Chem.* **1999**, *38*, 5988. (d) Mullins, C. S.; Pecoraro, V. L. *Coord. Chem. Rev.* **2008**, *252*, 416. (e) Christou, G. *Acc. Chem. Res.* **1989**, *22*, 328. (f) Mukhopadhyay, S.; Mandal, S. K.; Bhaduri, S.; Armstrong, W. H. *Chem. Rev.* **2004**, *104*, 3981. (g) Weatherburn, D. C.; Mandal, S.; Mukhopadhyay, S.; Bhaduri, S.; Lindoy, L. F. In *Comprehensive Coordination Chemistry II*; McCleverty, J. A.; Dilworth, J. R., Eds; Elesvier: Oxford, 2004; Vol. *5*, pp 91−109.

(2) (a) Sessoli, R.; Tsai, H.-L.; Schake, A. R.; Wang, S.; Vincent, J. B.; Folting, K.; Gatteschi, D.; Christou, G.; Hendrickson, D. N. *J. Am. Chem. Soc.* **1993**, *115*, 1804. (b) Christou, G.; Gatteschi, D.; Hendrickson, D. N.; Sessoli, R. *MRS Bull.* **2000**, *25*, 66. (c) Sessoli, R.; Gatteschi, D.; Ganeschi, A.; Novak, M. A. *Nature* **1993**, *365*, 141. (d) Gatteschi, D.; Sessoli, R. *Angew. Chem., Int. Ed.* **2003**, *42*, 268. (e) Aromi, G.; Brechin, E. K. *Struct. Bonding (Berlin)* **2006**, *122*, 1. (f) Kostakis, G. E.; Ako, A. M.; Powell, A. K. *Chem. Soc. Rev.* **2010**, *39*, 2238.

(3) (a) Manoli, M.; Johnstone, R. D. L.; Parsons, S.; Murrie, M.; Affronte, M.; Evangelisti, M.; Brechin, E. K. *Angew. Chem., Int. Ed.* **2007**, *46*, 4456. (b) Stamatatos, T. C.; Abboud, K. A.; Wernsdorfer, W.; Christou, G. *Angew. Chem., Int. Ed.* **2006**, *45*, 4134.

(4) Ako, A. M.; Hewitt, I. J.; Mereacre, V.; Clérac, R.; Wernsdorfer, W.; Anson, C. E.; Powell, A. K. *Angew. Chem., Int. Ed.* **2006**, *45*, 4926.

(5) Ge, C.-H.; Ni, Z.-H.; Liu, C.-M.; Cui, A.-L.; Zhang, D.-Z.; Kou, H.-Z. *Inorg. Chem. Commun.* **2008**, *11*, 675.

(6) (a) Moushi, E. E.; Stamatatos, T. C.; Wernsdorfer, W.; Nastopoulos, V.; Christou, G.; Tasiopoulos, A. J. *Inorg. Chem.* **2009**, *48*, 5049. (b) Nayak, S.; Lan, Y.; Clérac, R.; Hearns, N. G. R.; Wernsdorfer, W.; Anson, C. E.; Powell, A. K. *Dalton Trans.* **2009**, 1901.

(7) Nayak, S.; Evangelisti, M.; Powell, A. K.; Reedijk, J. *Chem.—Eur. J.* **2010**, *16*, 12865.

(8) (a) Christou, G. *Polyhedron* **2005**, *24*, 2065. (b) Gatteschi, D.; Sessoli, R.; Villain, J. *Molecular Nanomagnets*; Oxford University Press: New York, 2006.

(9) Waldmann, O.; Ako, A. M.; Güdel, H. U; Powell, A. K. *Inorg. Chem.* **2008**, *47*, 3486.

(10) (a) Boskovic, C.; Wernsdorfer, W.; Folting, K.; Huffman, J. C.; Hendrickson, D. C.; Christou, G. *Inorg. Chem.* **2002**, *41*, 5107. (b) Naskar, S.; Mishra, D.; Chattopadhyay, S. K.; Corbella, M.; Blake, A. J. *Dalton Trans.* **2005**, 2428.

(11) Ruiz, E.; Cauchy, T.; Cano, J.; Costa, R.; Tercero, J.; Alvarez, S. *J. Am. Chem. Soc.* **2008**, *130*, 7420.

(12) Ako, A. M.; Mereacre, V. M.; Clérac, R.; Hewitt, I. J.; Wernsdorfer, W.; Anson, C. E.; Powell, A. K. *Chem. Commun.* **2009**, 544.

(13) (a) Tang, J.; Hewitt, I. J.; Madhu, N. T.; Chastanet, G.; Wernsdorfer, W.; Anson, C. E.; Benelli, C.; Sessoli, R.; Powell, A. K. *Angew. Chem., Int. Ed.* **2006**, *45*, 1729. (b) Zheng, Y.-Z.; Lan, Y.; Anson, C. E.; Powell, A. K. *Inorg. Chem.* **2008**, *47*, 10813. (c) Hewitt, I. J.; Tang, J.; Madhu, N. T.; Anson, C. E.; Lan, Y.; Luzon, J.; Etienne, M.; Sessoli, R.; Powell, A. K. *Angew. Chem., Int. Ed.* **2010**, *49*, 6352. (d) AlDamen, M. A.; Clemente-Juan, J. M.; Coronado, E.; Marti-Gastaldo, C.; Gaita-Arino, A. *J. Am. Chem. Soc.* **2008**, *130*, 8874. (e) Xu, G.-F.; Wang, Q.-L.; Gamez, P.; Ma, Y.; Clérac, R.; Tang, J.-K.; Yan, S.-P.; Cheng, P.; Liao, D.-Z. *Chem. Commun.* **2010**, *46*, 1506. (f) Layfield, R. A.; McDouall, J. J. W.; Sulway, S. A.; Tuna, F.; Collison, D.; Winpenny, R. E. P. *Chem.—Eur. J.* **2010**, *16*, 4442.

(14) (a) Lin, P.-H.; Burchell, T. J.; Clérac, R.; Murugesu, M. *Angew. Chem., Int. Ed.* **2008**, *47*, 8848. (b) Hussain, B.; Savard, D.; Burchell, T. J.; Wernsdorfer, W.; Murugesu, M. *Chem. Commun.* **2009**, 1100. (c) Gamer, M. T.; Lan, Y.; Roesky, P. W.; Powell, A. K.; Clérac, R. *Inorg. Chem.* **2008**, *47*, 6581. (d) Ishikawa, N.; Sugita, M.; Ishikawa, T.; Koshihara, S.; Kaizu, Y. *J. Am. Chem. Soc.* **2003**, *125*, 8694. (e) Ishikawa, N. *Polyhedron* **2007**, *26*, 2147. (f) Guo, Y.-N.; Xu, G.-F.; Gamez, P.; Zhao, L.; Lin, S.- Y.; Deng, R.; Tang, J.; Zhang, H.-J. *J. Am. Chem. Soc.* **2010**, *132*, 8538. (g) Lin, P.-H.; Burchell, T. J.; Clérac, R.; Murugesu, M. *Angew. Chem., Int. Ed.* **2008**, *47*, 8848. (h) Rinehart, J. D.; Fang, M.; Evans, W. J.; Long, J. R. *Nat. Chem.* **2011**, *3*, 538.

(15) Mereacre, V.; Ako, A. M.; Clérac, R.; Wernsdorfer, W.; Hewitt, I. J.; Anson, C. E.; Powell, A. K. *Chem.—Eur. J.* **2008**, *45*, 707.

(16) (a) Li, M.; Lan, Y.; Ako, A. M.; Wernsdorfer, W.; Anson, C. E.; Buth, G.; Powell, A. K.; Wang, Z.; Gao, S. *Inorg. Chem.* **2010**, *49*, 11587. (b) Akhtar, M. N.; Zheng, Y.-Z.; Lan, Y.; Mereacre, V.; Anson, C. E.; Powell, A. K. *Inorg. Chem.* **2009**, *48*, 3015. (c) Mereacre, V. M.; Ako, A. M.; Clérac, R.; Wernsdorfer, W.; Filoti, G.; Bartolomé, J.; Anson, C. E.; Powell, A. K. *J. Am. Chem. Soc.* **2007**, *129*, 9248. (d) Abbas, G.; Lan, Y.; Mereacre, V.; Wernsdorfer, W.; Clérac, R.; Buth, G.; Sougrati, M. T.; Grandjean, F.; Long, G. J.; Anson, C. E.; Powell, A. K. *Inorg. Chem.* **2009**, *48*, 9345.

(17) (a) Novitchi, G.; Wernsdorfer, W.; Chibotaru, L. F.; Costes, J. P.; Anson, C. E.; Powell, A. K. *Angew. Chem., Int. Ed.* **2009**, *48*, 1614. (b) Schray, D.; Abbas, G.; Lan, Y.; Mereacre, V.; Sundt, A.; Dreiser, J.; Waldmann, O.; Kostakis, G. E.; Anson, C. E.; Powell, A. K. *Angew. Chem., Int. Ed.* **2010**, *49*, 5185.

(18) (a) Zaleski, C.; Depperman, E.; Kampf, J.; Kirk, M.; Pecoraro, V. *Angew. Chem., Int. Ed.* **2005**, *44*, 3912. (b) Mishra, A.; Wernsdorfer, W.; Abboud, K. A.; Christou, G. *J. Am. Chem. Soc.* **2004**, *126*, 15648. (c) Stamatotos, Th. C.; Teat, S. J.; Wernsdorfer, W.; Christou, G. *Angew. Chem., Int. Ed.* **2009**, *48*, 521. (d) Ferbinteanu, M.; Kajiwara, T.; Choi, K.-Y.; Nojiri, H.; Nakamoto, A.; Kojima, N.; Cimpoesu, F.; Fujimura, Y.; Takaishi, S.; Yamashita, M. *J. Am. Chem. Soc.* **2006**, *128*, 9008 and references cited therein. (e) Mishra, A.; Wernsdorfer, W.; Parsons, S.; Christou, G.; Brechin, E. K. *Chem. Commun.* **2005**, 2086. (f) Mishra, A.; Wernsdorfer, W.; Abboud, K. A.; Christou, G. *J. Am. Chem. Soc.* **2004**, *126*, 15648. (g) Aronica, C.; Pilet, G.; Chastanet, G.; Wernsdorfer, W.; Jacquot, J.-F.; Luneau, D. *Angew. Chem., Int. Ed.* **2006**, *45*, 4659 and references therein. (h) Langley, S. K.; Moubaraki, B.; Murray, K. S. *Dalton Trans.* **2010**, *39*, 5066. (i) Papatriantafyllopoulou, C.; Wernsdorfer, W.; Abboud, K. A.; Christou, G. *Inorg. Chem.* **2011**, *50*, 421. (j) Zou, L.-F.; Zhao, L.; Guo, Y.-N.; Yu, G.-M.; Guo, Y.; Tang, J.; Li, Y.-H. *Chem. Commun.* **2011**, *47*, 8659. (k) Iasco, O.; Novitchi, G.; Jeanneau, E.; Wernsdorfer, W.; Luneau, D. *Inorg Chem.* **2011**, *50*, 7373. (l) Baskar, V.; Gopal, K.; Helliwell, M.; Tuna, F.; Wernsdorfer, W.; Winpenny, R. E. P. *Dalton Trans.* **2010**, *39*, 4747. (m) Shiga, T.; Onuki, T.; Matsumoto, T.; Nojiri, H.; Newton, G. N.; Hoshino, N.; Oshio, H. *Chem. Commun.* **2009**, 3568. (n) Zeng, Y. -F.; Xu, G.-C.; Hu, X.; Chen, Z.; Bu, X.-H.; Gao, S.; Sanudo, E. C *Inorg. Chem.* **2010**, *49*, 9734. (o) Liu, J.-L.; Guo, F.-S; Meng, Z.-S.; Zheng, Y.-Z.; Leng, J.-D.; Tong, M.-L.; Ungur, L.; Chibotaru, L. F.; Heroux, K. J.; Hendrickson, D. N. *Chem. Sci.* **2011**, *2*, 1268. (p) Hołyńska, M.; Premužić, D.; Jeon, I.-R.; Wernsdorfer, W.; Clérac, R.; Dehnen, S. *Chem.—Eur. J.* **2011**, *17*, 9605.

(19) Brennan, S.; Cowan, P. L. *Rev. Sci. Instrum.* **1992**, *63*, 850.

(20) (a) Sheldrick, G. M. *SADABS (the Siemens Area Detector Absorption Correction)*; University of Göttingen, 1996. (b) Sheldrick, G. M. *SHELXTL 6.14*; Bruker AXS, Inc.: 6300 Enterprise Lane, Madison, WI 53719-1173, USA, 2003.
(21) van der Sluis, P.; Spek, A. L. *Acta Crystallogr.* **1990**, *A46*, 194.
(22) Boudreaux, E. A.; Mulay, L. N., Eds. *Theory and Applications of Molecular Paramagnetism*; Wiley: New York, 1976.
(23) Artacho, E.; Cela, J. M.; Gale, J. D.; García, A.; Junquera, J.; Martin, R. M.; Ordejón, P.; Sánchez-Portal, D.; Soler, J. M. *Siesta 3.0*; Fundación General Universidad Autónoma de Madrid, 2010.
(24) Artacho, E.; Sánchez-Portal, D.; Ordejón, P.; García, A.; Soler, J. M. *Phys. Status Solidi A* **1999**, *215*, 809.
(25) Soler, J. M.; Artacho, E.; Gale, J. D.; García, A.; Junquera, J.; Ordejón, P.; Sánchez-Portal, D. *J. Phys.: Condens. Matter* **2002**, *14*, 2745.
(26) Perdew, J.; Burke, K.; Ernzerhof, M. *Phys. Rev. Lett.* **1996**, *77*, 3865.
(27) Anisimov, V. I.; Aryasetiawan, F.; Lichtenstein, A. I. *J. Phys.: Condens. Matter* **1997**, *9*, 767.
(28) Kleinman, L.; Bylander, D. M. *Phys. Rev. Lett.* **1982**, *48*, 1425.
(29) Trouiller, N.; Martins, J. L. *Phys. Rev. B* **1991**, *43*, 1993.
(30) Ruiz, E.; Cauchy, T.; Cano, J.; Costa, R.; Tercero, J.; Alvarez, S. *J. Am. Chem. Soc.* **2008**, *130*, 7420.
(31) Ruiz, E.; Rodríguez-Fortea, A.; Tercero, J.; Cauchy, T.; Massobrio, C. *J. Chem. Phys.* **2005**, *123*, 074102.
(32) Ruiz, E.; Alemany, P.; Alvarez, S.; Cano, J. *J. Am. Chem. Soc.* **1997**, *119*, 1297.
(33) Ruiz, E.; Alvarez, S.; Cano, J.; Polo, V. *J. Chem. Phys.* **2005**, *123*, 164110.
(34) Ruiz, E. *Struct. Bonding (Berlin)* **2004**, *113*, 71.
(35) Ruiz, E.; Rodríguez-Fortea, A.; Cano, J.; Alvarez, S.; Alemany, P. *J. Comput. Chem.* **2003**, *24*, 982.
(36) Barandika, M. G.; Cortés, R.; Lezama, L.; Urtiaga, M. K.; Arriortua, M. I.; Rojo, T. *J. Chem. Soc., Dalton Trans.* **1999**, 2971.
(37) Shannon, R. D. *Acta Crystallogr.* **1976**, *A32*, 751.